Investigating the effects of temperature variation in vibration-based SHM

T.A. Dardeno [1], R.S. Mills [1], L.A. Bull [2], N. Dervilis [1], K. Worden [1]
[1] University of Sheffield, Department of Mechanical Engineering, Dynamics Research Group, Sheffield S1 3JD, UK

[2] The Alan Turing Institute,
The British Library, London NW1 2DB, UK

Abstract
Structural health monitoring (SHM), relies on evaluating certain features (e.g., natural frequencies), over time, to detect structural changes indicative of damage. However, damage-sensitive features often respond to benign variations in the environment, such as changes in temperature, as well as damage. These benign variations can mimic or mask damage, and can therefore affect the practical implementation and generalisation of SHM technologies. The aim of the current work is to investigate the effects of normal variation and identify methods to account for these changes. In this paper, an experimental campaign is discussed, in which vibration data were collected on two healthy, nominally-identical, full-scale composite helicopter blades. Testing was performed in a temperature-controlled chamber at temperatures between -20°C and 30°C, at increments of 5°C. Frosting tests were also performed on one of the blades to investigate the effects of ice accumulation. The frequency response functions of the blades were evaluated for changes in natural frequency.

1 Introduction

Cracking, corrosion, and other damage conditions can reduce structural stiffness, which can then manifest as a decrease in natural frequency. Natural frequency changes can also result from normal variations unrelated to damage. For example, an increase in ambient temperature or loosening of bolts at a support might reduce natural frequency and mimic a damaged state. An increase in mass can have a similar effect as a reduction in stiffness, and can also mimic damage (e.g., ice accumulation). Conversely, a change in environmental conditions that increases natural frequency, such as a decrease in ambient temperature, can mask reductions that are caused by damage. Because damage-sensitive features often respond to normal fluctuations as well as damage, distinguishing between damaged states and normal variations can be difficult, and can affect the practical implementation and generalisation of structural health monitoring (SHM) technologies [1, 2]. It is not usually feasible to collect comprehensive data that cover all possible variations affecting a given structure. Population-based SHM (PBSHM) can be used to make inferences among various members of a *population*, i.e., a group of similar systems [3, 4, 5, 6, 7].

In this work, vibration data were collected over a series of tests on two healthy, nominally-identical, full-scale composite helicopter blades. Testing was performed in a temperature-controlled chamber from -20 to 30 °C in increments of 5 °C. The effects of ice buildup on one of the blades were also investigated. This paper discusses how changes in the testing environment present as changes in the FRFs of the blades, specifically with respect to the locations of the peaks. In addition, preliminary research is presented regarding the development of a generalised normal condition for the helicopter blades using probabilistic regression models.

The layout of this paper is as follows. Section 2 describes the experiments performed on the blades, including the temperature variation tests (Section 2.1), and the ice accumulation tests (Section 2.2), and the

data collected. Section 3 then briefly introduces a generalised normal condition for the helicopter blades developed using an overlapping mixture of Gaussian processes.

2 Experiments

Vibration testing was performed on two healthy, nominally-identical, full-scale, composite helicopter blades in a temperature-controlled chamber at the Laboratory for Verification and Validation (LVV) in Sheffield, UK. The helicopter blades were tested in an approximate fixed-free boundary condition, with the blade root mounted on a fixture that was substantiated with a large concrete block.

A series of tests that considered the effects of temperature variation were conducted, where testing was performed at temperatures ranging from -20 to 30 °C in increments of 5 °C. In addition, the effects of frosting and ice accumulation on the blade dynamics were investigated. Temperature variation tests were performed on both helicopter blades, whereas frosting tests were completed on a single blade.

For all tests performed, data were collected using Siemens PLM LMS SCADAS hardware and software. Acceleration data were collected via ten uniaxial 100 mV/g accelerometers placed at various locations along the underside of each blade. An electrodynamic shaker provided a broadband excitation up to 400 Hz. The shaker was mounted to the bottom plate of the test fixture, and the shaker and force gauge were connected to the underside of the blades to excite the blades in the flapwise direction. A thermal jacket was used to protect the shaker when testing at lower temperatures. The sensor layout on each blade is shown in Figure 1.

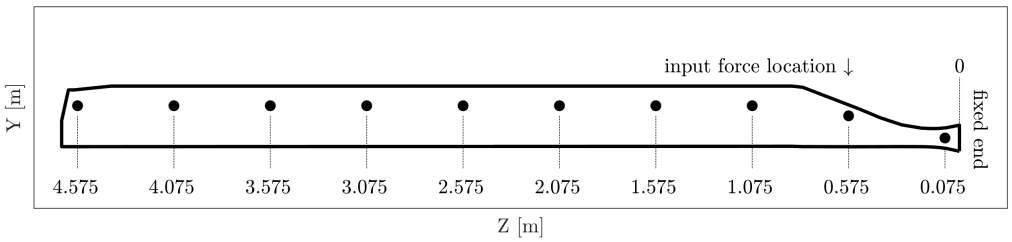

Figure 1: Sensor locations on helicopter blade.

2.1 Temperature Variation Tests

Ambient temperature affects stiffness, which can then alter the natural frequencies of a structure. This temperature dependence was demonstrated by performing vibration testing on two helicopter blades in an environmental chamber at various temperatures and computing FRFs. The FRFs were then investigated for changes in the positions of the peaks with respect to temperature.

2.1.1 Description of experiments

The temperature-controlled chamber was set to each of the temperatures of interest, after which the blades were allowed to soak for at least two hours to reach the desired temperature. Approximately 7.4 minutes of throughput force and acceleration data were collected for each test, with a time step of 1.25 x 10^{-3} seconds. The data were then divided into 20 blocks, each with 16384 samples. Some data at the start and end of the acquisition were discarded as they corresponded to powering up and down of the shaker. A Hanning window was applied to each data block and FRFs were computed in LMS. The FRFs were then averaged in the frequency domain. Data were collected over a relatively-long time period for each test and a large number of averages were used to improve the spectra at the lower modes, near the limits of the operating range of the sensors. The experimental setup is shown in Figure 2. Acquisition parameters are listed in Table 1.

Representative drive-point FRF and coherence spectra for the helicopter blades at 20 °C are shown in Figures 3a and 3b. (Note that the labels Blade 1 and Blade 4 are used for consistency with the results presented

in [8, 9]. In [8, 9], four helicopter blades, labeled Blades 1-4, were tested at ambient laboratory temperature, to investigate how differences in material properties, geometry, and boundary conditions can affect the dynamics of nominally-identical structures. Only Blades 1 and 4 were tested in the temperature-controlled chamber, and these results are presented in the current paper). Figures 3a and 3b show that the coherence was close to 1 at most of the resonances. Poor coherence was noted at the frequencies corresponding to the lower modes below 10 Hz. This difficulty in acquiring the first few modes resulted in part from the operating frequency range of the accelerometers and the extremely high flexibility of the blades, which limited the shaker placement. The spectra obtained at other sensor locations on the blade were of similar quality to those shown in Figures 3a and 3b.

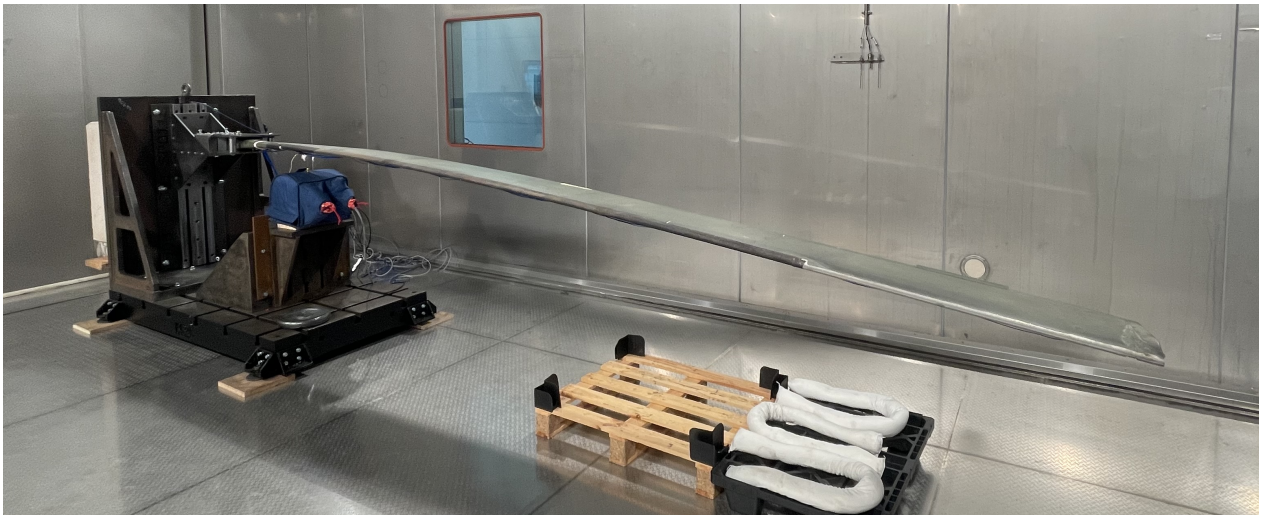

Figure 2: Helicopter blade in temperature-controlled chamber.

Table 1: Acquisition parameters.

Time step	1.25e-03
Acquisition time	20.48 s
Bandwidth	400 Hz
Lines	8192
Frequency step	4.88e-02 Hz
Window	Hanning

2.1.2 Discussion of experimental results

This discussion considers measurements obtained from the accelerometer closest to the blade tip; the feature changes visible in these measurements are representative of those at the other accelerometers. For Blade 1, the averaged FRF at each temperature is shown in Figures 4a and 4b, with Figure 4a showing the full measured bandwidth and Figure 4b showing only the mode at around 145 Hz. Likewise, for Blade 4, the averaged FRF at each temperature is shown in Figures 5a and 5b. A comparison of Blades 1 and 4 at the mode around 145 Hz is shown in Figure 6, for all temperatures tested.

Figures 4a and 5b show a proportional decrease in frequency corresponding to each incremental temperature increase, with discrepancies more noticeable at the higher modes than the lower modes. These results are expected, as the higher-frequency modes are more sensitive to environmental and other changes. For Blade 1, the maximum frequency difference among the tests was approximately 15.3 Hz (for modes less than 400 Hz), found in the band between 335 and 375 Hz, as obtained via peak-picking. In the same band, the average frequency difference for each 5 °C increment was approximately 1.5 Hz. For the mode at

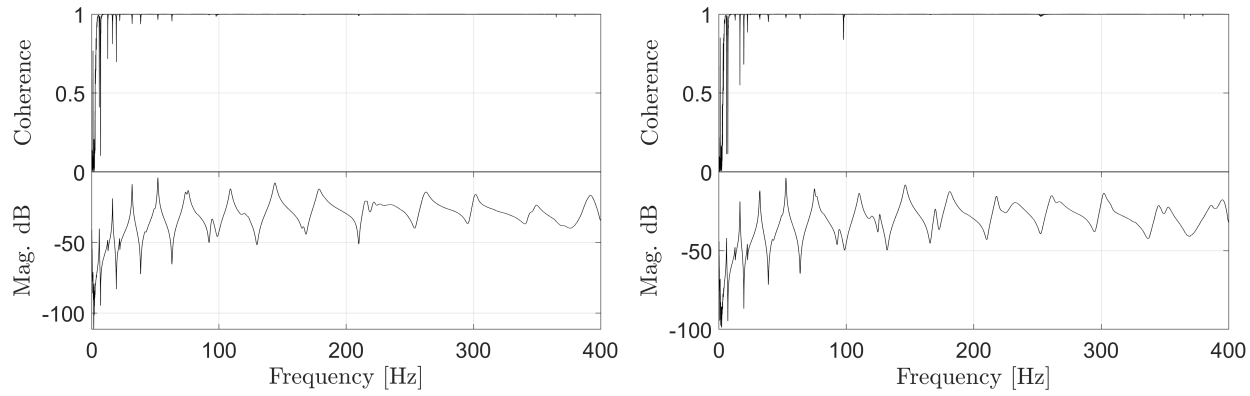

Figure 3: Representative coherence and FRF from (a) Blade 1 and (b) Blade 4.

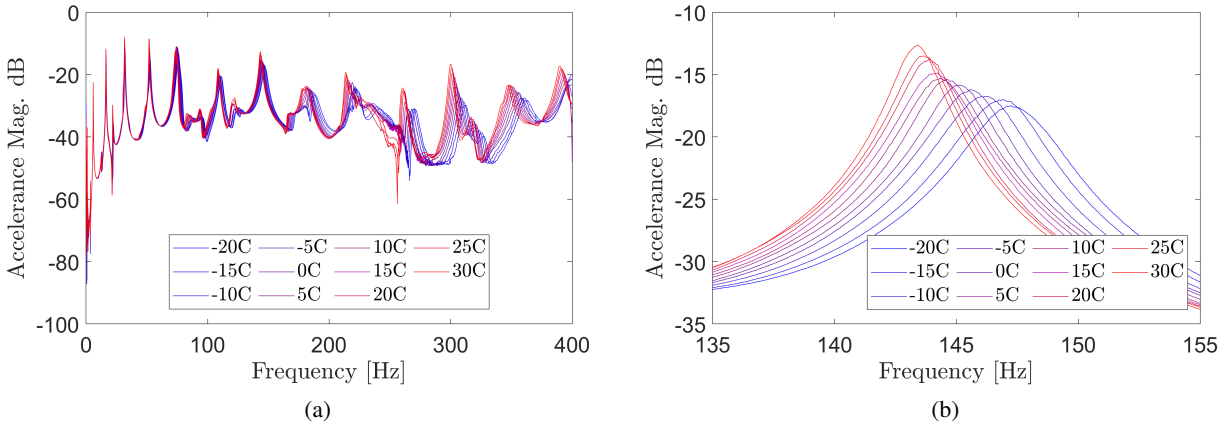

Figure 4: FRF magnitudes from -20 to 30 °C for Blade 1, a) 0 to 400 Hz and (b) 135 to 155 Hz.

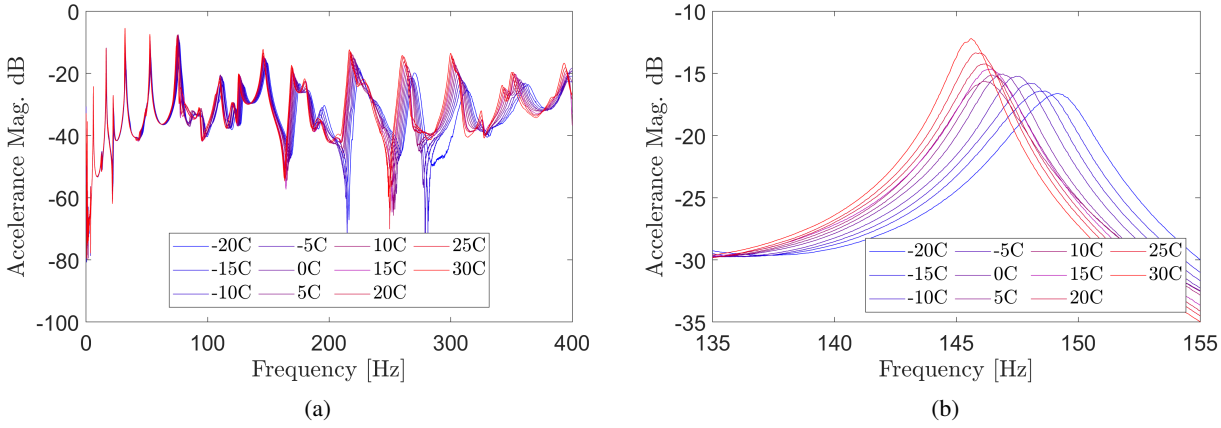

Figure 5: FRF magnitudes from -20 to 30 °C for Blade 4, a) 0 to 400 Hz and (b) 135 to 155 Hz.

approximately 145 Hz shown in Figure 4b, the maximum frequency difference was approximately 3.8 Hz, and the average frequency difference for each 5 °C increment was approximately 0.38 Hz. Likewise, for

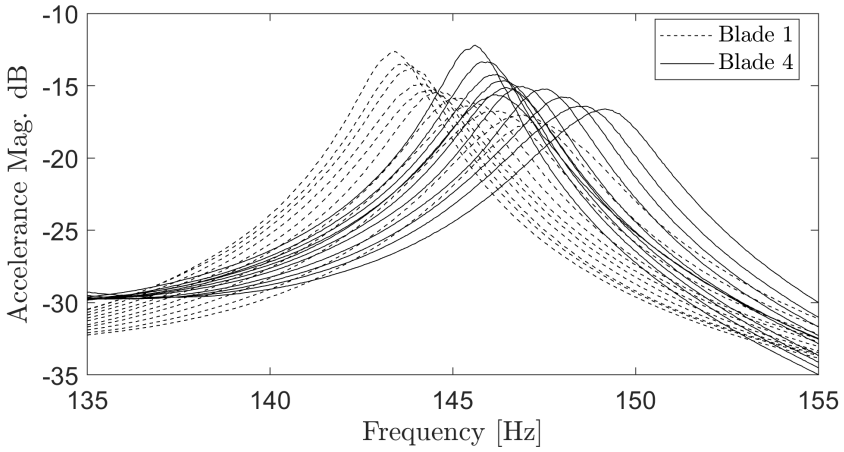

Figure 6: FRF magnitudes at all temperatures for Blades 1 and 4, 135 to 155 Hz.

Blade 4, the maximum frequency difference among the tests was approximately 12.4 Hz for modes less than 400 Hz, found in the band between 335 and 375 Hz. In the same band, the average frequency difference for each 5 °C increment was approximately 1.2 Hz. For the mode at approximately 145 Hz shown in Figure 5b, the maximum frequency difference was approximately 3.6 Hz, and the average frequency difference for each 5 °C increment was approximately 0.40 Hz.

Figure 6 shows that Blade 4 tends to be slightly higher in frequency than Blade 1, as visible in the peak between 135 Hz and 155 Hz. (Indeed, at 20 °C, the difference in frequency between the blades is approximately 1.8 Hz.) However, there is considerable overlap of the peaks depending on the temperature of the testing environment, demonstrating the significance of environmental conditions (in addition to variations in material properties and boundary conditions [8, 9]) in developing a normal condition for a population of structures.

2.2 Ice Accumulation Tests

A decrease in temperature increases the stiffness of a structure, which increases natural frequency. However, ice accumulation increases mass, which can decrease natural frequency depending on the amount and location of the ice buildup. To investigate the effects of ice accumulation on helicopter-blade dynamics, frosting tests were performed on Blade 1 and FRFs were inspected for changes in the peak positions after three incremental ice buildups.

2.2.1 Description of experiments

The temperature-controlled chamber was set to -20 °C and the blade was allowed to acclimate for at least two hours. Plastic sheeting was hung from a gantry towards the root of the blade to protect the shaker from water spray and ice accumulation, and a plastic sheet was wrapped around the shaker to provide additional protection. Each accelerometer was fitted with a custom, 3D-printed protective shell. Icing control was performed in LabView, and thermocouples were used to monitor blade temperature.

The blade was sprayed with water from six nozzles, resulting in ice accumulation that spanned more than half the blade length starting from the tip. Buildup occurred in three increments, each corresponding to a total spray mass of approximately 4.6 kg, 6.6 kg, and 8.6 kg, respectively [1]. Ice accumulation following the

[1]It is unknown how much ice accumulated on the blade for each test, but preliminary testing showed that roughly 0.66 kg of ice accumulated on the blade for a spray mass of 5.37 kg, or 0.12 kg of ice buildup for each 1 kg of water spray. This estimate was determined by allowing ice to accumulate on a detachable film, placing the film and ice in a bucket, and then finding the total weight. The film and bucket were then dried and weighed again, with the difference giving the mass of ice. However, these values may not accurately reflect what occurred during the actual tests, as buildup may have occurred differently on the detachable film

final buildup is shown in Figure 7.

Figure 7: Helicopter blade during ice accumulation tests.

Measurements were taken following each incremental buildup, with spraying paused during the measurements. The same acquisition settings used during the temperature variation tests (as shown in Table 1), were used to collect vibration data during the icing tests.

2.2.2 Discussion of experimental results

FRFs for a baseline (no ice accumulation) test at -20 °C and the three buildup tests are shown in Figures 8a and 8b, where Figure 8a shows the full measured 400 Hz bandwidth and Figure 8b shows a reduced bandwidth from 0 to 80 Hz. As with the temperature-variation tests, this discussion considers measurements obtained from the accelerometer closest to the blade tip when looking at frequency shifting.

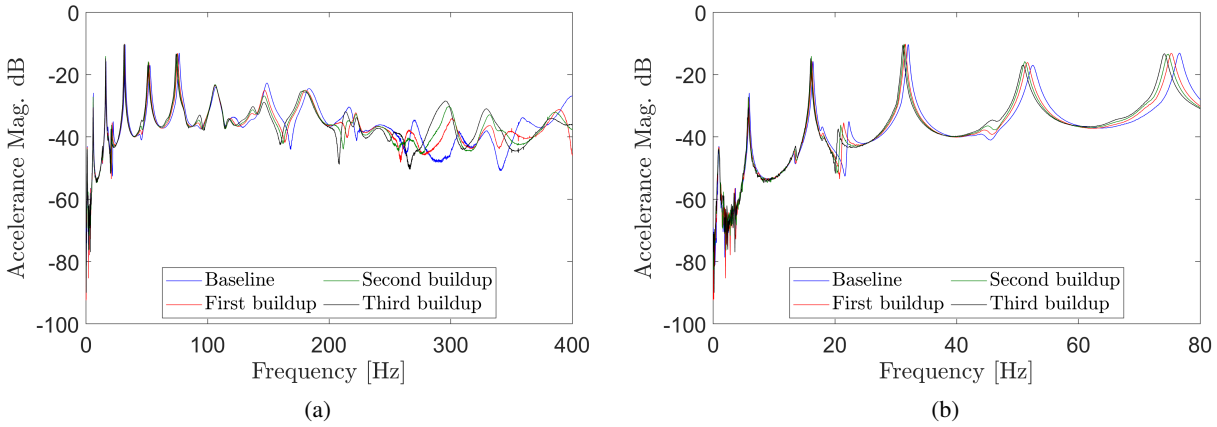

Figure 8: FRF magnitudes for incremental ice accumulation on Blade 1, a) 0 to 400 Hz and (b) 0 to 80 Hz.

Figures 8a and 8b show a decrease in frequency corresponding to each incremental buildup of ice, and the decrease appears proportional to the amount of spray used in the buildup. While the temperature variation tests showed a global effect in the FRFs (i.e., the entire blade was subjected to a temperature change), the ice accumulation was not consistent across the blade. As such, the extent that each mode was affected depends

compared to the blade surface.

on the location and amount of ice relative to the nodes and antinodes of a given mode. The largest frequency differences that can reasonably be discerned via peak-picking occurred between 280 and 320 Hz, at a 6.1 Hz reduction for the first build up (compared to baseline), an 8.6 Hz reduction for the second buildup, and an 11.1 Hz reduction for the third buildup. For the modes below 80 Hz, the largest frequency differences occurred at the mode near 75 Hz, with a 1.3 Hz reduction for the first build up (compared to baseline), a 1.9 Hz reduction for the second buildup, and a 2.4 Hz reduction for the third buildup.

The effect on mode shapes was then considered for a subset of the bending modes below 80 Hz (found at approximately 6 Hz, 16 Hz, 31 Hz, 51 Hz, and 75 Hz). The Modal Assurance Criterion (MAC) [10] was computed for each of the buildups relative to the baseline measurements. The MACs are shown in Table 2. An overlay plot of the bending mode at 75 Hz from the baseline measurements with the same mode after the third ice buildup is shown in Figure 9.

Table 2: Modal Assurance Criterion (MAC) for each incremental ice buildup relative to baseline.

		Baseline				
		6 Hz	16 Hz	31 Hz	51 Hz	75 Hz
Buildup 1	6 Hz	100	0.1	0	0.1	0
	16 Hz	0	99.9	0	0	0.2
	31 Hz	0	0	100	0	0.2
	51 Hz	0	0	0.1	99.8	0.3
	75 Hz	0	0.1	0.2	1.2	99.7
Buildup 2	6 Hz	100	0.2	0	0.1	0
	16 Hz	0	99.8	0.1	0	0.3
	31 Hz	0	0	99.9	0	0.1
	51 Hz	0	0	0.2	99.5	0.1
	75 Hz	0	0.1	0.2	1.5	99.2
Buildup 3	6 Hz	99.9	0.3	0	0.3	0
	16 Hz	0	99.4	0.1	0	0.5
	31 Hz	0	0	99.8	0.2	0.1
	51 Hz	0	0	0.2	98.9	0
	75 Hz	0	0.1	0.2	2	98.5

Figure 9: 75 Hz mode from the baseline test plotted in overlay with the same mode from the third ice buildup.

Although the diagonal MAC values were found to decrease with each buildup, the change in MAC for the mode shapes considered was quite low. Indeed, the lowest MAC occurred at the mode around 75 Hz, but 98.5 is still considered good correlation for many applications [11]. Further investigation into local effects may be warranted, but could require a higher sensor density or additional sensor types (e.g., strain gauges).

3 Development of a Population Form

This work has used Gaussian process regression (GP) to model the population form for four nominally-identical helicopter blades at ambient laboratory temperature [8, 9], to account for differences in material properties/geometry among the blades and variations in boundary conditions. A continuation of this research involving the temperature effects discussed in the current paper is ongoing. A preliminary form for Blade 1 using data collected at a subset of the temperatures tested (-20 °C through 30 °C, in increments of 10 °C) was developed using an overlapping mixture of Gaussian processes (OMGP), as shown in Figures 10a and 10b. An OMGP allows for unsupervised learning of the population form while taking into account variations among the data across the input space. Relevant OMGP theory can be found in [7, 8, 12]. Additional techniques to account for these temperature variations (such as cointegration and transfer learning) are also being considered.

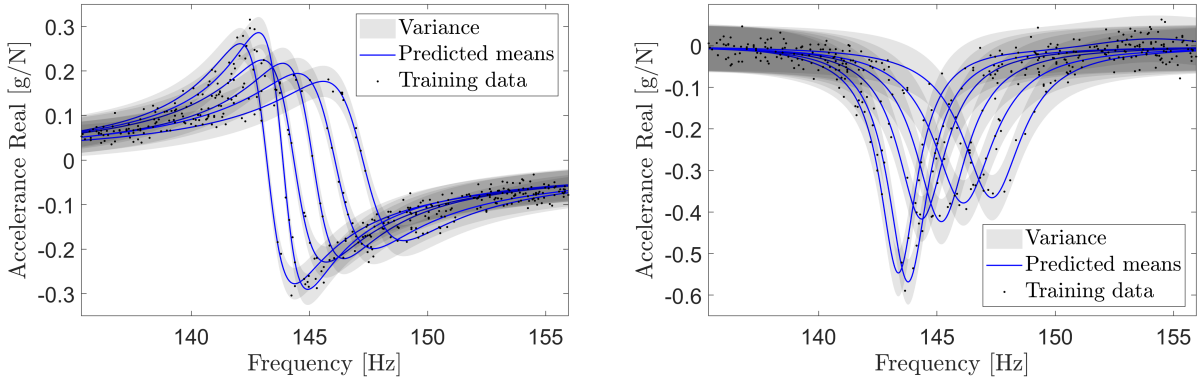

Figure 10: Population form for Blade 1 using (a) real and (b) imaginary FRF data at -20 °C, -10 °C, 0 °C, 10 °C, 20 °C, and 30 °C.

4 Conclusions

This paper presented the results of an experimental campaign, where vibration data were collected on two healthy, nominally-identical, full-scale composite helicopter blades in a temperature-controlled chamber. The first set of tests involved taking measurements at various temperatures, while the second tests investigated the effects of ice accumulation. The FRFs of the blades were evaluated for changes in natural frequency resulting from these environmental variations. For the temperature variation tests, examination of FRFs showed that an average frequency difference of approximately 1.5 Hz occurred for each 5 °C incremental change in frequency. For the icing tests, the largest discernible frequency reductions were as high as 11.1 Hz resulting from the added mass. These findings are important for the implementation and generalisation of SHM systems that may depend on monitoring the effects of damage-related stiffness reduction. Accounting for normal variations is especially important for PBSHM, which seeks to transfer valuable information, such as normal operating conditions and damage states, across similar structures.

5 Acknowledgements

The authors gratefully acknowledge the support of the UK Engineering and Physical Sciences Research Council (EPSRC), via grant references EP/R003645/1 and EP/R004900/1. L.A. Bull was supported by Wave 1 of the UKRI Strategic Priorities Fund under the EPSRC grant EP/W006022/1, particularly the *Ecosystems of Digital Twins* theme within that grant and the Alan Turing Institute.

This research made use of The Laboratory for Verification and Validation (LVV), which was funded by the EPSRC (grant numbers EP/J013714/1 and EP/N010884/1), the European Regional Development Fund (ERDF) and the University of Sheffield. The authors would like to extend special thanks to Michael Dutchman, for assisting with experimental setup.

References

[1] K. Worden, H. Sohn, and C. Farrar, "Novelty detection in a changing environment: Regression and interpolation approaches," *J. Sound Vib.*, vol. 258, pp. 741–761, 2002.

[2] H. Sohn, "Effects of environmental and operational variability on structural health monitoring," *Philos. Trans. A: Math. Phys. Eng. Sci.*, vol. 365, pp. 539–560, 2007.

[3] L.A. Bull, P.A. Gardner, J. Gosliga, T.J. Rogers, N. Dervilis, E.J. Cross, E. Papatheou, A.E. Maquire, C. Campos, and K. Worden, "Foundations of population-based SHM, Part I: Homogeneous populations and forms," *Mech. Syst. Signal Process.*, vol. 148, p. 107141, 2021.

[4] L.A. Bull, T.J. Rogers, N. Dervilis, E.J. Cross, and K. Worden, "A Gaussian process form for population-based structural health monitoring," in *Proceedings of the 13th International Conference on Damage Assessment of Structures (DAMAS 2019), Porto, Portugal*. Springer, July 9-10, 2019.

[5] J. Gosliga, P.A. Gardner, L.A. Bull, N. Dervilis, and K. Worden, "Foundations of population-based SHM, Part II: Heterogeneous populations–graphs, networks, and communities," *Mech. Syst. Signal Process.*, vol. 148, p. 107144, 2021.

[6] P.A. Gardner, L.A. Bull, J. Gosliga, N. Dervilis, and K. Worden, "Foundations of population-based SHM, Part III: Heterogeneous populations–mapping and transfer," *Mech. Syst. Signal Process.*, vol. 149, p. 107142, 2021.

[7] L.A. Bull, P.A. Gardner, T.J. Rogers, N. Dervilis, E.J. Cross, E. Papatheou, A.E. Maquire, C. Campos, and K. Worden, "Bayesian modelling of multivalued power curves from an operational wind farm," *Mech. Syst. Signal Process.*, p. 108530, 2021.

[8] T. A. Dardeno, L. A. Bull, R. S. Mills, N. Dervilis, and K. Worden, "Modelling variability in vibration-based PBSHM via a generalised population form," preprint, 2022.

[9] T.A. Dardeno, L.A. Bull, N. Dervilis, and K. Worden, "Investigating experimental repeatability and feature consistency in vibration-based SHM," in *Proceedings of the 13th International Workshop on Structural Health Monitoring (IWSHM)*, 2022.

[10] R. J. Allemang, "A correlation coefficient for modal vector analysis," in *Proc. 1st Int. Modal Analysis Conference*, 1982, pp. 110–116.

[11] R.J. Allemang, A.W. Phillips, and D.L. Brown, "Autonomous modal parameter estimation: statisical considerations," in *Modal Analysis Topics, Volume 3*. Springer, 2011, pp. 385–401.

[12] M. Lázaro-Gredilla, S. Van Vaerenbergh, and N.D. Lawrence, "Overlapping mixtures of Gaussian processes for the data association problem," *Pattern Recognit.*, vol. 45, no. 4, pp. 1386–1395, 2012.